Influence of natural and anthropogenic activities on UV Index variations – a study over tropical urban region using ground based observations and satellite data

**K. V. S. Badarinath · Shailesh Kumar Kharol ·
V. Krishna Prasad · Anu Rani Sharma · E. U. B. Reddi ·
H. D. Kambezidis · D. G. Kaskaoutis**

Abstract Measurements of total ozone column and solar UV radiation under different atmospheric conditions are needed to define variations of both UV and ozone and to study the impact of ozone depletion at the Earth's surface. In this study, spectral and broadband measurements of UV-B irradiance were obtained along with total ozone observations and aerosol optical depth measurements in the tropical urban region of Hyderabad, south India. We specifically used an Ultra-Violet Multifilter Rotating Shadow band Radiometer (UVMFR-SR), to measure UV irradiance in time and space. To assess the aerosol and O_3 effects on ground-reaching UV irradiance, we used measurements from a Microtops II sun photometer in addition to the Tropospheric Ultraviolet Visible radiation (TUV) model. We also assessed the Defense Meteorological Satellite Program – Operational Line Scanner (DMSP-OLS) night time satellite data for inferring biomass burning fires during the study period. Results clearly suggested a negative correlation between the DMSP-OLS satellite derived fire count data and UVMFR-SR data suggesting that aerosols from biomass burning are directly attenuating UV irradiance in the study region. Also, correlation analysis between UV index and ozone measurements from sun photometer and TOMS-Ozone Mapping Instrument (OMI) indicated a clear decrease in ground reaching UV-B irradiance

K. V. S. Badarinath (✉) · S. Kumar Kharol · A. Rani Sharma
Department of Space, Atmospheric Science Section, National Remote Sensing Agency,
Government of India, Balanagar, Hyderabad 500 037, India
e-mail: badrinath_kvs@nrsa.gov.in

V. Krishna Prasad
Agroecosystem Management Program, The Ohio State University, Columbus, OH, USA

E. U. B. Reddi
Department of Environmental Sciences, Andhra University, Visakhapatnam 530 003, India

H. D. Kambezidis · D. G. Kaskaoutis
Atmospheric Research Team, Institute for Environmental Research and Sustainable Development,
National Observatory of Athens, Lofos Nymphon, P.O. Box 20048, 11810 Athens, Greece

D. G. Kaskaoutis
Department of Physics, Laboratory of Meteorology, University of Ioannina, 45110 Ioannina, Greece

during higher ozone conditions. The higher levels are attributed to photochemical production of O_3 during the oxidation of trace gases emitted from biomass burning. Results also suggested a relatively high attenuation in UV irradiance (~6% higher) from smoke particles than dust. We also found a relatively good agreement between the modeled (TUV) and measured UV irradiance spectra for different atmospheric conditions. Our results highlight the factors affecting UV irradiance in a tropical urban environment, south India.

1 Introduction

Although ultraviolet radiation reaching the earth's surface constitutes only a small fraction of the total radiant solar energy, understanding ultraviolet (UV) radiation characteristics is extremely important, because it has important influence on atmospheric chemistry (Iqbal 1983). Also, UV radiation reaching the ground has adverse biological and environmental effects. The UV region of the spectrum is subdivided mainly into UV-C (200–280 nm), UV-B (280–315 nm) and UV-A (315–400 nm). The UV-C component is completely absorbed by atmospheric constituents such as oxygen and ozone. The UV-B region is strongly dominated by ozone absorption while the UV-A radiation is weakly affected by ozone. The UV radiation relevant to environmental biology is restricted to the combined UV-B and UV-A ranges (Madronich 1993). Most importantly, recent knowledge of stratospheric ozone depletion has led to concerns about increased levels of biologically harmful UV-B (280–315 nm) radiation reaching the Earth's surface, relative to UV-A (315–400 nm) radiation. Increased UV-B surface irradiance can lead to damage to both terrestrial and oceanic organisms, and increases in the incidences of cataracts and skin cancer in humans (McKenzie et al. 1998; Udelhofen et al. 1999). Also, if the amount of UV radiation is sufficiently high, the self-protection ability of some biological species is exhausted and the subject may be severely damaged. The need to reach the public with simple-to-understand information about UV and its possible detrimental effects led scientists to define a parameter that can be used as an indicator of the UV exposures. This parameter is called the UV index. It is related to the well known erythemal effects of solar UV radiation on human skin and it has been defined and standardized under the umbrella of several international institutions such as World Meteorological organization (WMO), World Health Organization (WHO), United Nations Environment Program (UNEP), etc. The UV Index (UVI) is now widely used in many operational weather reports and forecasts. In Europe, for example, there are more than a dozen forecasting centers that release estimated UVI values for countries or regional areas.

The diurnal and annual variability of solar UV radiation reaching the ground is governed by astronomical and geographical parameters as well as by the atmospheric conditions. The most important factors affecting the UV radiation reaching the Earth's surface are atmospheric ozone, solar zenith angle, aerosols, altitude, atmospheric scattering, cloud cover and surface albedo (Meloni et al. 2004). For example, clouds and atmospheric aerosols have been found to attenuate UV radiation and are believed to mask the increase of UV irradiance due to stratospheric ozone depletion (Frederick et al. 1993; Meleti and Cappellani 2000). The influence of aerosols on the transmission of UV radiation has important consequences for stratospheric and tropospheric photochemistry, human and plant biology, remote sensing of column ozone, and surface UV mapping. The effect of tropospheric aerosols on UV radiation varies widely in time and space due to their short

residence time (2–7 days), variability in size, shape, and chemical composition, and dependence on relative humidity (Reuder and Schwander 1999). The magnitude of the net aerosol effect can be large (over certain parts of the Earth, aerosols can reduce the UV irradiance at the surface by more than 50%; Krotkov et al. 1998) and is highly variable, depending on the number of particles and their physical and chemical properties. Uncertainties in aerosol particle microphysical data, can cause variability of up to 10% in predictions of actinic flux and UV irradiance (Früh et al. 2003). Studies have been conducted at continental sites in North America (DeLuisi 1997; Kerr 1997) and in Europe (Krzyscin and Puchalski 1998; Cañada et al. 2000) which shows how aerosol optical depth and aerosol characteristics can affect UV irradiance. For example, Balis et al. (2004) have shown from a co-located Raman lidar system and spectral UV-B irradiance measurements that for the same AOD and for the same ozone column, surface UV-B irradiances may differ by up to 10%, which was attributed to differences in aerosol type. In addition, some modeling studies (Diaz et al. 2000) have suggested that aerosol vertical (height) distribution can also affect surface UV irradiances by 2–5% for optical depth observations at visible wavelengths. Due to the combined involvement of different aerosol parameters in controlling UV levels, it is difficult to determine accurately the role of each parameter. Nevertheless, it is important to understand the effects that aerosols have on surface UV irradiances. New studies demonstrated the strong influences of variations in aerosol concentration and composition on long- and short-term variations in surface UV radiation. Some of the studies include Chubarova (2002) for Moscow, Russia; Barnard et al. (2003) for California, USA; Palancar and Toselli (2002) for Cordoba, Argentina; Micheletti et al. (2003) for Buenos Aires, Argentina; Ogunjobi and Kim (2004) for Kwangju, South Korea; Arola et al. (2003) for Sodankylä, Finland, and Thessaloniki, Greece; Kambezidis et al. (2005) for Athens, Greece, and di Sarra et al. (2002) and Meloni et al. (2003a,b,c, 2005) for the island of Lampedusa in the Mediterranean, Kambezidis et al. (2005) for Athens, Greece, Jaroslawski and Krzyscin (2005), at Belsk, Poland, etc.

In contrast to several of the above UVI, aerosol and ozone monitoring studies conducted all over the world in varied urban environments, relatively few studies have been conducted in the study region of Hyderabad, south India (Badarinath et al. 2007a). The primary objective of this study is to characterize spatio-temporal variations in UVI in Hyderabad, south India. Intensive ground measurements have been conducted to analyze the effects of dust and anthropogenic aerosols (from biomass burning) on ground reaching UV irradiance, in addition to satellite data analysis. We also assessed the correlation between ozone variation and the amount of UV radiation that penetrates the atmosphere to reach the earth's surface. Also, comparison between the measured direct-beam UV irradiance and the Tropospheric Ultraviolet Visible radiation (TUV) model has been made to evaluate the influence of ozone and atmospheric aerosols on UV radiation. In summary, this study attempts to improve the current understanding of UVI, aerosols and ozone in a typical urban environmental setting in south India. Our study also represents 'first of the kind' integrated study utilizing satellite remote sensing data, ground measurements and TUV model for characterizing UVI variations in the study area.

2 Study area

The study area of Hyderabad is located between 17°10′ and 17°50′ N latitude and 78°10′ and 78°50′ E longitude (Badarinath et al. 2007a). Hyderabad is the fifth largest city of India, highly urbanized with population of 5,751,780 inhabitants (census 2001). The city is

influenced not only by urban pollutants but also by industrial as well as neighboring biomass-burning trace gases and aerosols. The climate of the region is semi-arid with a total rainfall of ~700 mm occurring mostly during the monsoon season in the June–October period. The climatology of the area experiences four dominant seasons each year, winter (December–February), pre-monsoon (March–May), monsoon (June–August), and post-monsoon (September–November). The measurements for this work were carried out under clear-sky conditions in the premises of the National Remote Sensing Agency (NRSA) campus located at Balanagar (17°28′ N and 78°26′ E), Hyderabad, located well within the urban center.

3 Data and methodology

3.1 Ground-based measurements

The UV measurements were taken from ground-based instruments, as well as estimates derived from satellite radiance measurements. The principal instruments used in this study are an Ultraviolet Multifilter Rotating Shadow band radiometer (UV-MFRSR), a MICRO-TOPS-II sun photometer and a UV-meter.

The UVMFR-SR was deployed at National Remote Sensing Agency (NRSA) campus, Balanagar, Hyderabad, India and the data is collected from January to April, 2006. The UVMFR-SR works under the same principles as the original visible wavelength version described in Harrison et al. (1994) and is detailed in Bigelow et al. (1998). This instrument measures both total and diffuse irradiance for four specified wavelengths (299, 304.7, 310.8, and 317.1 nm) with a 2 nm nominal full width at half maximum (FWHM) bandwidth. Measurements of total and diffuse irradiance were recorded every 2 min interval. There is filter-to-filter variation in the nominal wavelength center (±0.5 nm), and each is characterized to an accuracy of ±0.02 nm as described by Gao et al. (2001). The direct beam is obtained by subtraction of the diffuse horizontal from the total horizontal irradiance and includes the corrections described by Harrison et al. (1994). The cosine response and irradiance calibration of the UVMFR-SR were conducted (Yankee Environmental Systems) in spring 1999 before deployment to the field site.

The Solar Light microprocessor-controlled total ozone portable spectrometer (MICRO-TOPS-II) was used to measure the aerosol optical depth (AOD) at the wavelengths 380, 440, 500, 675, 870 and 1,020 nm (Morys et al. 2001) as well as the total column ozone. The instrument measures the irradiance signals at different wavelengths in mV, from which the absolute irradiance in W m^{-2} is obtained by multiplying the signal with the calibration factor (W m^{-2} mV^{-1}). The calibration relies on a high-performance voltage reference with the temperature coefficient ≤0.001% per degree Celcius and long-term stability of ~0.005% per year. The long-term stability of the UV filter is better than 0.1 nm year^{-1}, while the accuracy of the sun-targeting angle is better than 0.1° and the FWHM is 2.4±0.4 nm. In order to avoid any errors in sun-targeting angle, the MICROTOPS-II was mounted on a tripod stand throughout the experimental period. The sun photometer works on the principle of measuring the solar radiation intensity at the specified wavelengths and converts it to optical depth by knowing the corresponding intensities at the top of the atmosphere (TOA). The TOA irradiances at each wavelength were calculated via the well-known Langley method, while the Kasten and Young's (1989) expression for the air mass was used. The whole procedure for the AOD derivation is described in Badarinath et al. (2007b). The MICROTOPS-II sun photometer also measures the total ozone-column amount. The instrument measures the

direct-beam component at three wavelengths: one strongly absorbed by ozone, second moderately absorbed, and third not absorbed. By comparing the calculated theoretical extinction of light of the direct-beam with the measured values at multiple wavelengths of solar irradiance, the ozone amount is inferred.

A UV-meter from Solar Light Co., USA has been used to measure UV in the spectral range of 280–320 nm in units of minimum erythema dose per hour (MED h^{-1}). This unit is calculated by the cross-multiplication of the irradiance flux in the UV-B spectral range and the Erythema Action spectra (McKinlay and Diffey 1987). The effective power of 1 MED h^{-1} is equalent to 0.583 W m^{-2} for a MED of 21 mJ cm^{-2}. This effective power of 1 MED was utilized to convert the measured UV-B radiation to W m^{-2} when calculating the corresponding clearness and UV indexes. The UV-meter measurements were performed under cloudless conditions covering the period January–April, 2006. The cosine response of the instrument is ±5% with a resolution of 0.01 MED h^{-1}. The measurement technique employed in this instrument utilizes colored glass filters and a highly stable UV-sensitive fluorescent phosphor to stop all of the sun's visible light and convert UV photons into visible light, which in turn is measured by a solid-state photo detector. In order to obtain the required accuracy, the UV sensors are temperature stabilized to +40°C using a heating element. The linearity is within ±2% over the normal range of operation. The time sampling of the instrument is one measurement per second. The measurements were corrected for deviation from the CIE action spectrum.

Further, the Tropospheric Ultraviolet Visible (TUV) radiation model (Madronich 1993) was used to obtain the direct-beam solar irradiance at 299, 304.7, 310.8, and 317.1 nm. The major input parameters required to run this model are the columnar ozone (in DU), the AOD at 550 nm, single scattering albedo, apart from other parameters, such as altitude. The measured ozone values from MICROTOPS-II were used as input to TUV model. The AOD value at 550 nm was calculated by extrapolating the AOD value at 500 nm (measured from MICROTOPS-II) using the Angstrom exponent α (Singh and Singh 2004). A surface albedo value of 0.05 was used for all the model calculations. The altitude parameter was set to 500 m for Hyderabad. The UV spectral irradiance calculations were then done for the direct-beam component at all four UV-MFRSR wavelengths. As reported by Singh and Singh (2004), the change in surface albedo values had no effect on the direct-beam irradiance estimated from the model, since it only affects the multiple scattering between surface and atmosphere.

3.2 UV Index

The UVI is determined by weighting the incident solar radiation at the Earth's surface with the erythemal response of human skin in the 280–400 nm band obtained by the UV-meter, and then summing over this wavelength range to derive the total effect. It is given as:

$$\text{UVI} = 40/\text{W m}^2 \int_{280}^{400} E(\lambda)A(\lambda)d(\lambda)$$

where, $E(\lambda)$ is the irradiance at wavelength λ and $A(\lambda)$ is the (dimensionless) CIE (Commission Internationale de l'Eclairage) action spectrum (McKinlay and Diffey 1987). One UVI unit is equivalent to biologically effective solar UV radiation of 0.025 W m^{-2}. The UVI can be reported as a continuous measure but the most common value reported is the maximum UVI for each day. A UVI of 3–5 is considered "moderate," a UVI of 8–10 is

"very high," and a UVI greater than 10 is "extreme" (WHO 2002). In addition, Dahlback (1996) has described a method to derive biologically effective UV dose rates from irradiance measurements with moderate bandwidth filter instruments that have only a few channels in the UV band. Using this technique, Bhattarai et al. (2007) obtained UVI in Kathmandu, Nepal, while those results are compared with the present ones.

3.3 Satellite data

To infer the forest fire characteristics over the Indian region, daily data sets from the Defense Meteorological Satellite Program – Operational Line Scanner (DMSP-OLS) were assessed from February to April 2006, for monitoring nighttime fire products. DMSP operates in sun-synchronous orbits with nighttime overpasses ranging from about 7 P.M. to 10 P.M. local time with a swath width of 3,000 km. The OLS is an oscillating scan radiometer with two spectral bands. The visible band-pass straddles the visible and near-infrared portion of the spectrum (0.5 to 0.9 μm) and the thermal band-pass covers the 10.5–12.5 μm region. The low-light sensing capabilities of the OLS at night permit the measurement of radiances down to 10^{-9} W cm^{-2} sr^{-1}. Fires present at the Earth's surface at the time of the overpass of the DMSP are readily detected in the visible band. Extensive details relating to DMSP satellite sensor are discussed in Elvidge et al. (1997).

In addition, we also analyzed the ozone data from the Ozone Monitoring Instrument (OMI). The Ozone Monitoring Instrument (OMI) is the Dutch-Finnish contribution to the NASA EOS-Aura platform, which was launched in July 2004. OMI is the first of a new generation of UV-visible space-borne spectrometers that use two-dimensional detectors. These detectors enable OMI to daily observe the entire Earth with small ground pixel size (13×24 km^2 at nadir), which makes the instrument suitable for tropospheric composition research and detection of air pollution at urban scales. The scientific objectives of OMI concern the recovery of the ozone layer, tropospheric pollution, the contribution of tropospheric ozone and aerosols to climate change and changes in surface UV-B (Levelt et al. 2006a, b). The ozone and UVI values derived by OMI were compared with the measured ones in order to check the validity of the satellite sensors. Further, surface measurements of Ozone were carried out using O_3 analyser 41M of Environment S.A. (Badarinath et al. 2007a).

4 Results and discussion

4.1 Comparison between ground-based and satellite retrievals

The variation of ozone, UVI and AOD values from January to April, 2006 are shown in Fig. 1a–d. The ozone values constitute the mean daily amount measured from MICRO-TOPS-II instrument, the UVI and the AOD are refers to the mean daily value. The UVI values are strongly associated with the zenith angle, ozone content and aerosol loading. They are lower in winter and maximum in spring. As a consequence, the greatest effect on UV dose is due to ozone amount and aerosol load. The highest UVI values occurred in the period 9–21th March (68–80 Julian days), when the AOD is low and the ozone amount was significantly lower than the fore coming days. The UVI can reach even at 7.0 on clear-sky days. The observed values are relatively higher than the UVI values reported for some sites in UK (UVI~2.4, Gies et al. 2004) and less than those reported at Darwin, Australia (UVI~ 9.0–10.1, Kalashnikova et al. 2007). Also, Bhattarai et al. (2007) reported a UVI as high as

7.8 for solar zenith angle of 36.8° in Kathmandu, Nepal. The UVI values in Nepal are strongly dependent on aerosol loading and zenith angle. The UVI in the present study area seem to be in the moderate-to-high scale. These inferences clearly suggest a strong need to conduct systematic UVI measurements covering different regions in India, as UVI values are expected to be even higher in the summer, which can have deleterious effects on humans and ecosystems. Ozone content showed similar values in the first ~80 days of 2006 (till 20 March) with values below 250 DU. A rapid increase in Ozone (DU) were observed in the beginning of April, while in the rest of this month the ozone values remained relatively high (above 280 DU). The AOD at both wavelengths (380 and 500 nm) showed similar pattern with increasing values towards spring. Some of the peaks observed in the AOD can be attributed to additional aerosol load from natural sources (biomass-burning or desert-dust aerosols), since the anthropogenic emissions are continuous in this urban environment.

The correlation between OMI and MICROTOPS-II ozone values is shown in Fig. 2. It is worth to be noticed that the ground-based retrievals refer only to the common dates and at the time of OMI overpass above the study region, thus the slight differences between the MICROTOPS-II ozone values between Figs. 1 and 2. The sudden variations in ozone and AOD after Julian day 80 were attributed to increased biomass burning due to forest fires over the region. The trends in ozone variations from Microtops and OMI are matching. The sudden raise observed in Microtops measured ozone compared to OMI was attributed to the fact that Microtops provides point observations as compared to 125×100 km grid average value of OMI. As a consequence the data in Fig. 2 are lesser, 79 against 92 in Fig. 1. A linear fit, associated with (80%) of the variance, shows a relative good agreement between satellite and ground-based measurements (lower panel). Nevertheless, ozone values

Fig. 1 a–d Julian day variations of UV Index (a), columnar ozone from MICROTOPS-II (b), Aerosol Optical Depth (AOD) at 380 nm (c) and AOD at 500 nm (d) over the region. The UVI corresponds to the noontime 1-h averaged value, while the other parameters refer to mean daily values
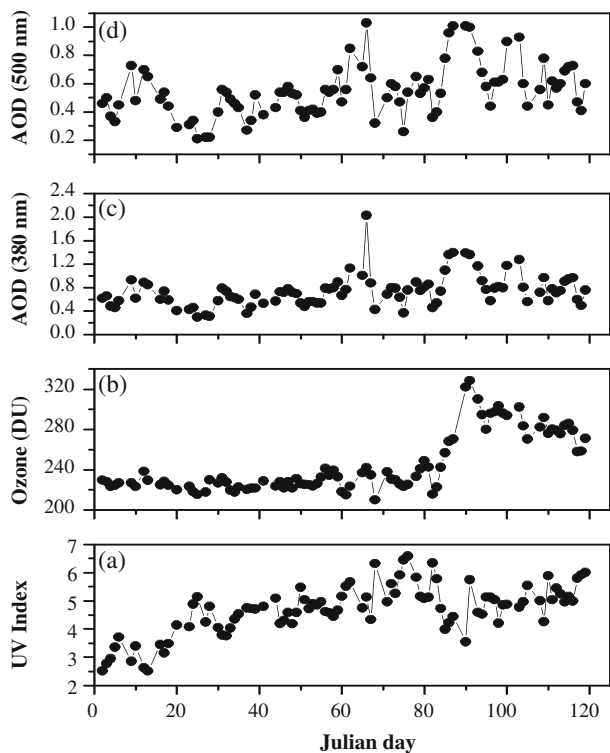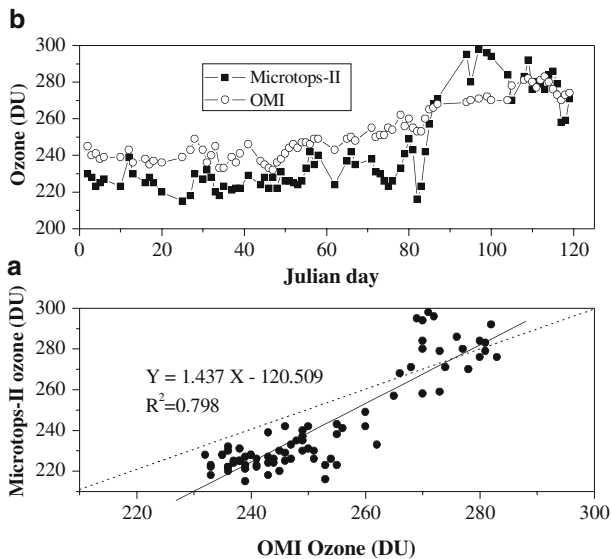
Fig. 2 a–b Correlation (a) and
Julian day variation (b) between
the ozone values derived by
MICROTOPS-II ozonometer and
OMI satellite. Only the common
dates are used in the relationship.
The MICROTOPS-II values cor-
respond to values near the OMI
overpass

obtained by OMI are in general higher than the respective MICROTOPS-II, exhibiting an average difference of ~4% relative to OMI data. It is observed that ozone values derived by OMI are systematically higher than those of MICROTOPS-II, with the exception of few days in the end of the measuring period (upper panel). The mean OMI-ozone value is 253 ± 15 DU against to 242 ± 24 DU derived by MICROTOPS-II. Similar to our studies, little higher ozone values from satellites have been also reported by Bhattarai et al. (2007) for February 2005 in Kathmandu, Nepal. Possible reasons for the discrepancies between satellite and ground-based measurements may be related to the instrument calibration and the differences in the spatial resolution. In addition, temporal differences can also occur because of difference in timing as well as changing atmospheric conditions (Bhattarai et al. 2007).

4.2 Influence of aerosols

Among the several factors influencing UVI, clouds constitute by far the most important factor and can introduce high variability in surface UV irradiance (McKenzie et al. 2007). The whole data set used in this study was obtained under cloudless conditions and, therefore, the effect of clouds on UV irradiance could not be evaluated. Apart from clouds, aerosol and ozone concentrations can modify the UV-B levels significantly at surface. In the preceding section, aerosol effects on UVI were examined followed by the influence of ozone.

Biomass burning is identified as a major source of atmospheric pollution, giving rise to the release of large quantities of gaseous emissions (black carbon, organic carbon) and particulate matter (Badarinath et al. 2007b). SO_2 is also a minor biomass-burning product (Andreae and Merlet 2001). Some studies reported that biomass-burning processes in forest areas surrounding Hyderabad have large impact on solar radiation (Kharol and Badarinath 2006; Badarinath et al. 2007b). The variation of DMSP-OLS fire counts in the measurement period is plotted against UVI derived from ground measurements (Fig. 3). As expected, there is an increasing trend in UVI values from January to April due to the higher sun elevation, while the largest UVI values were observed in the middle of March. The low UVI values on certain days (e.g. around 57th, 85th and 92nd Julian days)

Fig. 3 Julian day variations of UV Index and DMSP-OLS derived nighttime fire counts. The UVI corresponds to mean daily values associated with the standard deviations presented by the *vertical bars*
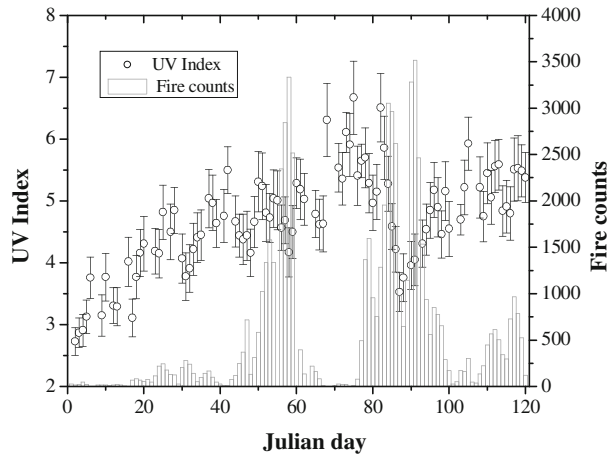
correlated well with large forest-fire counts over the region. This is also confirmed by ground measurements of aerosol optical properties (with high $AOD_{500} \sim 1.0$) and corresponding columnar ozone (~320 DU) measurements from the sun photometer (see also Fig. 1). The lower UVI values associated with the large number of forest-fire counts are confirmed by Fig. 4, which provides the scatter plot of fire counts with the UVI derived from the ground based UV-meter. In this figure, only fire counts above 1,000 are presented, while the fire counts and UVI values were grouped in order to reduce the high scatter. The inverse correlation between fire counts and UVI suggests that aerosols from biomass burning are directly attenuating UV irradiance. Fire counts could explain nearly 50% of UVI variability ($R^2 = 0.51$) in the study region.

To evaluate the impact of aerosols on UVI, the AOD measurements derived from MICROTOPS-II were correlated with the ground measured UVI values. Figure 5 shows the scatter plots of UVI and AOD at 380 (upper panel) and 500 nm (lower panel). The AOD data corresponds to the same hour with the UVI values, i.e., around local noon and, therefore, only measurements for clear skies at this time interval are used. The results suggest a strong negative correlation between UVI and AOD, nearly independent from the wavelength, thus stressing the attenuation of UV radiation by aerosols.

Spectral UV irradiance measurements obtained from UV-MFRSR in four spectral bands centered at 299, 304.7, 310.8 and 371.1 nm under different atmospheric conditions, 16 March 2006 (clear-sky day), 31 March 2006 (biomass-burning day) and 10 April 2006 (dusty day) are shown in Fig. 6a–d. These days are mostly devoid of clouds, except of some minor cloud occurrence on 31 March 2006, between 13:00 and 13:40. These figures clearly reveal the attenuation of UV irradiance in all spectral bands caused by biomass-burning aerosols and dust particles on 31st March 2006 and 10th April 2006, respectively, compared to that on 16 March 2006 (clear-sky day). The analysis of the data sets suggests a mean daily reduction of 22%, 49%, 72%, and 38% on 31 March 2006 (smoke $AOD_{500} \sim 1.07$) and 16%, 44%, 68%, and 29% on 10 April 2006 (dust $AOD_{500} \sim 0.86$) at the respective wavelengths 299, 304.7, 310.8 and 371.1 nm as compared to 16 March 2006 (clear sky $AOD_{500} \sim 0.25$). These results also suggest the strong influence of smoke on UV-B radiation. From the measurements, a reduction of ~40–50% in UV-B was found on burning day, while on dusty day the reduction was ~35–40%. These findings are closer to the estimates (40–50% reduction at 299 to 300 nm) given by Kalashnikova et al. (2007) during

Fig. 4 Scatter plot of DMSP-OLS derived nighttime fire counts and UV Index. Both DMSP-OLS and UV Index are gathered for 50–100 fire counts

$Y = 6.22345 - 6.2445E-4\ X$

$R^2 = 0.51$
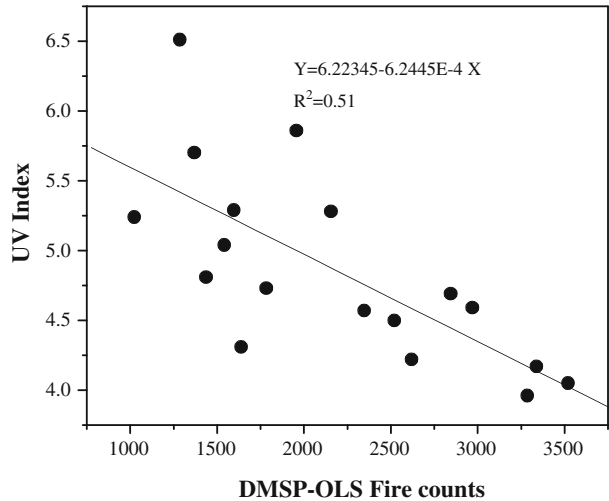
smoke aerosols over Darwin, Australia. Therefore, the larger decreases in UV irradiance caused by biomass-burning aerosols compared to desert dust, is attributed to the higher AOD_{500} on 31 March 2006 and to the more intense irradiance attenuation caused by fine-mode aerosols at the shorter wavelengths (Schuster et al. 2006). In recent studies over Hyderabad, Badarinath et al. (2007b) found a ~24% decrease in $UV_{(ery)}$ amount caused by biomass-burning aerosols, while Kharol and Badarinath (2006) reported a 12.5 W m^{-2} decrease in solar irradiance (400–1,100 nm) per 0.1 increase in AOD value. In the three days considered above, the ozone effect cannot be ignored since the measured ozone amounts on 31 March and 10 April are significantly higher (320 and 294 DU, respectively) than that on 16 March (225 DU). This fact is more depicted at 304.7 and 310.8 nm, where the ozone absorption coefficient is higher. The differences in sun elevation between the three days may have a slight effect on the computed reductions, but these differences are of

Fig. 5 a–b Scatter plots of UV Index and MICROTOPS-II derived Aerosol Optical Depth (AOD) at 380 (**a**) and 500 nm (**b**). Both UVI and AOD values correspond to noontime
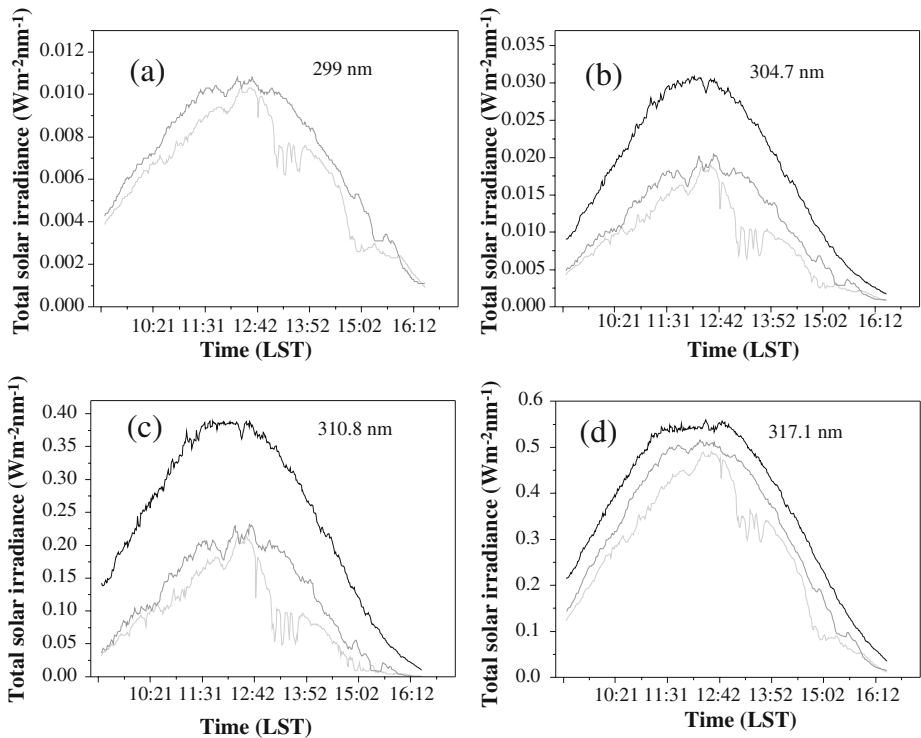

$Y = -2.25859X + 6.93417$

$R^2 = 0.80$

(a)

$Y = -2.94322X + 6.86674$

$R^2 = 0.73$

(b)
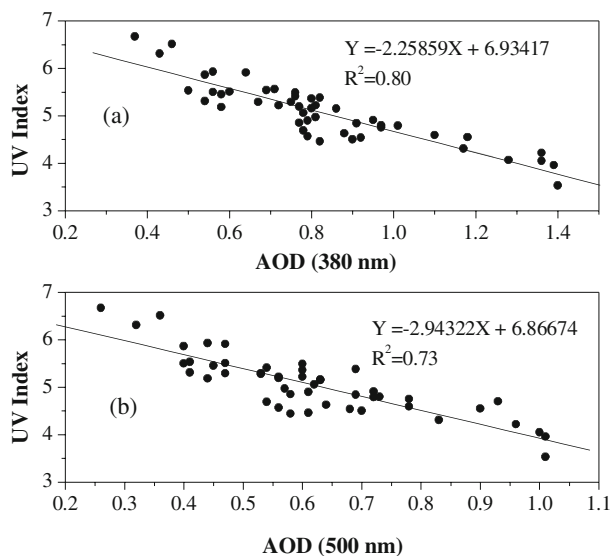
Fig. 6 a–d Diurnal variations in total solar irradiance at 299- (**a**), 304.7- (**b**), 310.8- (**c**) and 317.1-nm (**d**) at different atmospheric conditions, normal-day (16 March 2006, *black*), biomass-burning day (31 March 2006, *light grey*) and dusty-day (10 April 2006, *grey*)

minor importance for daily averaged values. Thus, the solar zenith angle range on 16 March is between 20° and 56°, on 31 March between 14° and 52° and on 10 April between 10° and 55°.

4.3 Tropospheric ozone

Factors, such as clouds, aerosols and surface albedo do not have the strong wavelength dependence like ozone on the attenuation of ground-reaching UV radiation (Bhattarai et al. 2007). Ozone is produced indirectly in the atmosphere through photochemical reactions, if there are enough precursors and UV radiation. Then, under favorable photochemistry conditions, ozone-rich air masses can be transported to long distances from the source region influencing the radiation field. Higher levels of tropospheric ozone are attributed to photochemical production during the oxidation of trace gases emitted by biomass burning (Lelieveld and Dentener 2000). A scatter plot between measured ozone concentration and DMSP-OLS nighttime fire counts over the region (Fig. 7a), with a relatively good correlation coefficient ($R^2=0.50$) confirms these findings. Note that for fire counts above 1000 the ozone concentration is always above 50 ppb. As a direct consequence, the tropospheric ozone production during the biomass-burning episodes strongly affects the columnar ozone amount, as clearly revealed from the good correlation ($R^2=0.83$) between surface ozone concentration and ozone columnar amount (Fig. 7b). These findings are in agreement with Pace et al. (2005), who found elevated concentrations of CO and O_3 in biomass-burning plumes, in Mediterranean regions. In contrast, SO_2 did not show clear

Fig. 7 a–b Scatter plot of DMSP-OLS derived nighttime fire counts and surface ozone concentration measured from ozone analyzer (**a**), and correlation of measured ozone surface concentration with column ozone amount derived from MICROTOPS-II (**b**)
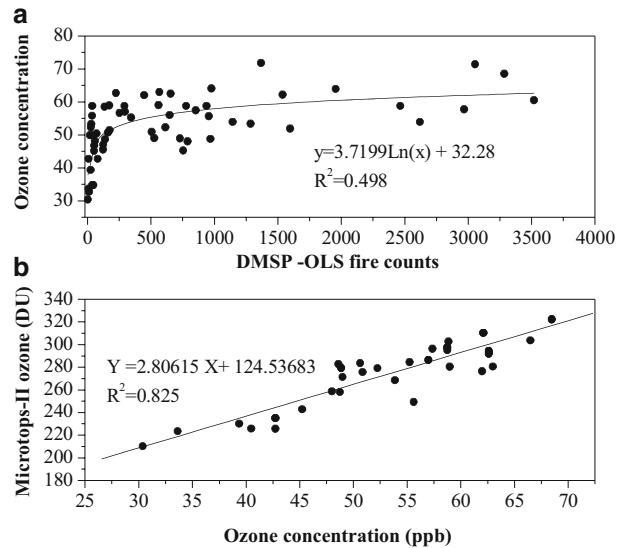
trend. Also, O_3 amounts during biomass-burning periods are mainly affected by synoptic systems through horizontal advection and large-scale vertical motions (di Sarra et al. 2002; Pace et al. 2005).

Absorption in the UV-B region may be primarily attributed to ozone and to a lesser extent to SO_2, NO_2 and other minor species (McKenzie et al. 2007). Figures 8a,b show the scatter plot of UVI (derived from the UV-meter) and ozone measured from MICROTOPS-II sun photometer and OMI instrument, respectively. UVI are 1-h averaged values close to OMI overpass. The negative correlations between UVI and ozone from both types of measurements suggest a clear decrease in UV-B radiation under higher ozone conditions. The inverse correlation between the total ozone column and the UV irradiance observed in this study, were also reported by other researchers elsewhere (Harris et al. 1997; di Sarra et al. 2001b). However, the scatter of the data points in our case is high, since the UVI is closely related to the aerosol load and aerosol optical properties. Comparing the Figs. 5a,b and 8a,b, it is concluded that the UVI values in the urban environment of Hyderabad are strongly related to the atmospheric turbidity, as a consequence weaker correlations were observed between UVI values and ozone amount.

4.4 Comparison with the TUV model

We utilized TUV model to predict the direct-beam UV irradiance under different atmospheric conditions. The TUV model was run for three different atmospheric conditions i.e., on 31st March 2006 (biomass-burning day), 16th March 2006 (normal day) and 10th April 2006 (dusty day). The modeled irradiances were recorded from morning to afternoon, with a step of 1 h, for all the above dates. The TUV model inputs include the solar zenith angle on the exact time of the measurements, the ozone value derived from MICROTOPS-II, the AOD_{550}, the Angstrom exponent and the single scattering albedo. The AOD_{550} and the Angstrom exponent values were obtained from the calculated AOD values, while appropriate values for the single scattering albedo were used, aiming at the best performance between measured and modeled values. The Figs. 9a–d show the scatter plots of measured and

Fig. 8 Scatter plot of UV Index
and Ozone measured from
MICROTOPS-II Ozonometer (a)
and OMI-satellite (b). In the
lower panel (a) the ozone and
UVI values refer to noontime,
while in *upper panel* (b) the UVI
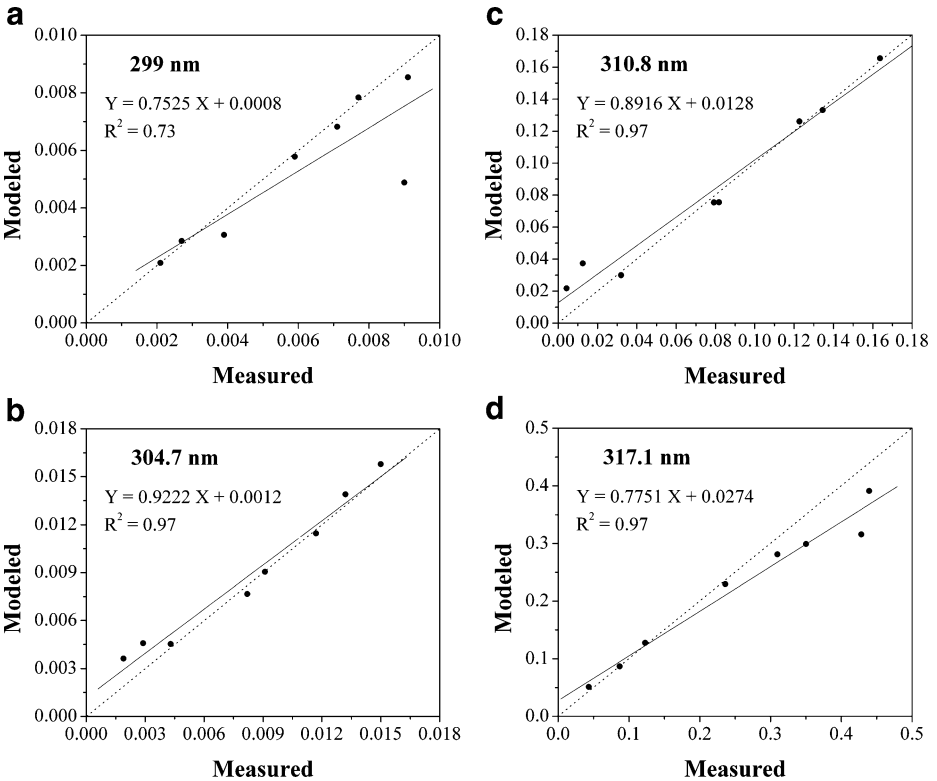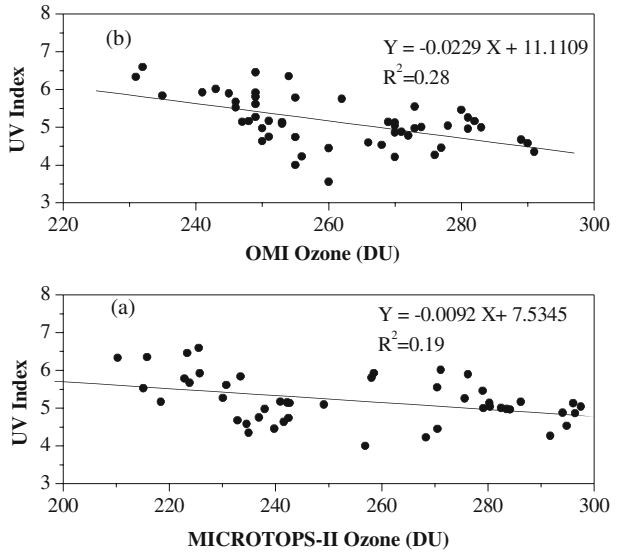corresponds to values near the
OMI overpass

Fig. 9 **a–d** Correlation between measured and modeled direct-beam UV irradiance at four spectral bands (299, 304.7, 310.8, 317.1 nm) on 31 March 2006 (burning day)

modeled direct-beam UV irradiances at four wavelengths (299, 304.7, 310.8 and 317.1 nm) on 31 March 2006 (burning day). On this day the modeled and measured UV irradiance followed similar trend but there is large scatter especially at lower wavelengths (299 nm) with correlation (R^2=0.73) as compared to longer wavelengths (R^2=0.97 for 304.7, 310.8 and 317.1 nm, respectively). The irradiances calculated by the model at 299 nm are particularly lower than the measured values, while the irradiances estimated from the TUV model at 304.7, 310.8 and 317.1 nm had higher accuracy. At all wavelengths, the uncertainties between measured and modeled irradiances are considerably lower, thus highlighting the ability of the model to simulate the irradiances under such smoke-turbid conditions. The single scattering albedo values used in this day were in the range of 0.89 to 0.95.

On dusty day (Fig. 10a–d) the TUV model exhibited the same behavior as before in all wavelengths. For the better performance, relatively low (0.86–0.87) single scattering albedo values were used for this case. These values correspond to well-absorbing dust particles, or to a well-mixed aerosol field with the local emissions of black carbon, which can be very high under turbid conditions in Hyderabad (Badarinath et al. 2007a).

The TUV model showed better performance in remote high-altitudes sites of Northern India (Singh and Singh 2004). The TUV application in the Northern India concludes to similar underestimation and overestimation of the measured irradiances for wavelengths lower and higher to 310 nm, respectively (Singh and Singh 2004). The better performance in these areas may be attributed to the more transparent atmospheric conditions, since for each radiative transfer model the greater uncertainties caused by the input parameters
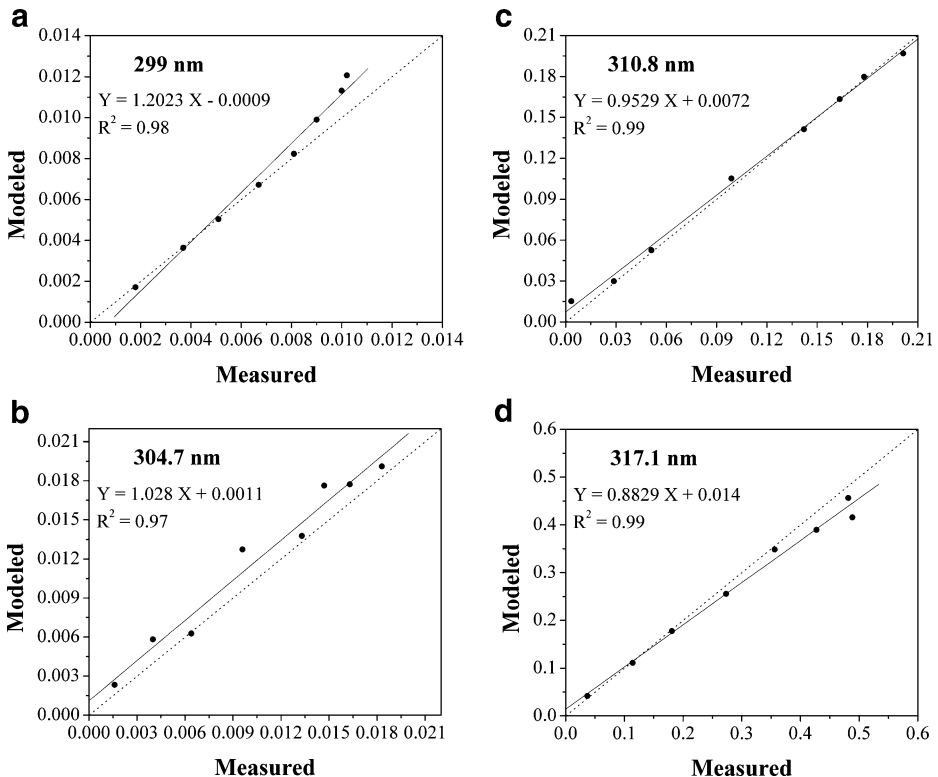

Fig. 10 a–d Same as in Fig. 9, but for on 10 April 2006 (dusty day)

corresponding to aerosol load and optical properties. Therefore, in low turbid conditions the solar irradiance can be accurately simulated by the radiative transfer models, as recently found by Kaskaoutis and Kambezidis (2008). These suggestions are also confirmed by the present applications, since the agreement between measured and modeled UV irradiances is much better under low turbid conditions, Fig. 11. High values of single scattering albedo (0.98–0.99) were used for the best model application. These values correspond to nearly absolutely scattering particles like sulphur, which can be found in large quantities is Hyderabad area (Anjaneyulu et al. 2005). However, on this clear sky day, the anthropogenic emissions and black carbon concentrations are low, and, therefore, the urban atmosphere approaches to rural characteristics, with single scattering albedo values near to 0.98. Further, at UV wavelengths, the diffuse component of radiation is also important and should be considered while understanding the influence of anthropogenic activities.

5 Conclusions

The influence of aerosols and ozone on UV radiation and its controlling factors were characterized in the typical urban environment of Hyderabad, south India. In addition to aerosols and ozone clouds also play an important role in attenuating ground reaching solar irradiance. Several ground-based measurements including UV-MFRSR, UV-meter, MICROTOPS-II sun photometer and satellite data were used to infer the UV radiation
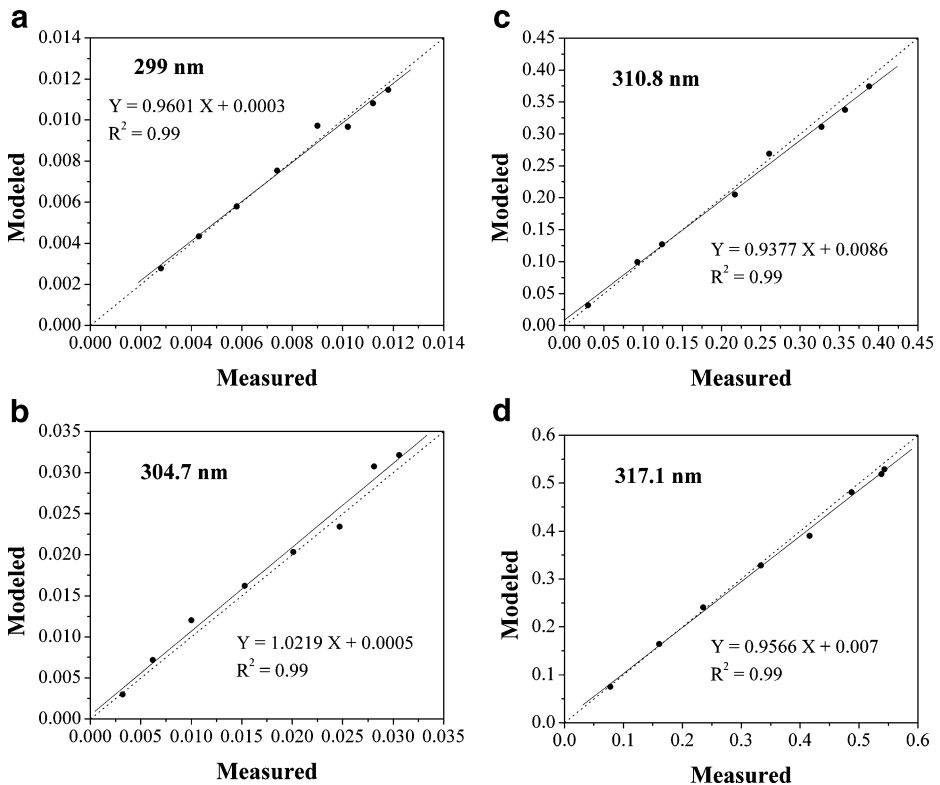

a 299 nm
$Y = 0.9601 X + 0.0003$
$R^2 = 0.99$

b 304.7 nm
$Y = 1.0219 X + 0.0005$
$R^2 = 0.99$

c 310.8 nm
$Y = 0.9377 X + 0.0086$
$R^2 = 0.99$

d 317.1 nm
$Y = 0.9566 X + 0.007$
$R^2 = 0.99$

Fig. 11 **a–d** Same as in Fig. 9, but for on 16 March 2006 (normal day)

characteristics. A correlation analysis between the AOD values obtained from MICRO-TOPS-II and UVI and ozone measurements from both MICROTOPS-II and Ozone Monitoring Instrument (OMI) were used to understand the attenuation of UV radiation. A detailed analysis of the UV irradiance at four wavelengths (299, 304.7, 310.8, and 317.1 nm measured from UV-MFRSR) was also presented. DMSP-OLS nighttime fire data sets were analyzed to understand the influence of anthropogenic aerosols on ozone production and on UV attenuation. The results from this study suggest that:

- In addition to urban pollutants, aerosols from biomass burning play a significant role on surface UV-B radiation.
- The negative correlation between UV Index values and fire counts obtained by DMSP-OLS suggested further reduction in surface UV radiation caused by smoke particles. In addition the relationship between UV Index and aerosol optical depth shows a strong negative correlation.
- A reduction in UV irradiance on 31 March 2006 ($AOD_{500}{\sim}1.07$) was almost 6% stronger than that on 10th April 2006 ($AOD_{500}{\sim}0.86$), suggesting relatively higher attenuation of UV radiation from smoke than dust particles.
- The inverse correlation between UV Index and ozone measurements from MICROTOPS-II and Ozone Monitoring Instrument (OMI) shows a clear decrease in UV-B during higher ozone conditions. The higher levels are attributed to photochemical production of O_3 during the oxidation of trace gases emitted by biomass burning from neighboring regions.
- The TUV model can be used over urban areas to obtain the direct-beam irradiance values in the UV band only under clear-sky conditions. This is supported by relatively good agreement between TUV-modeled values and UV-MFRSR measurements at different wavelengths.

References

Andreae, M.O., Merlet, P.: Emission of trace gases and aerosols from biomass burning. Global Biogeochem. Cycles **15**, 955–966 (2001)

Anjaneyulu, A., Jayakumar, I., Hima Bindu, V., Sagareswar, G., Rao, P.V.M., Rambabu, N., Ramani, K.V.: Use of multi-objective air pollution monitoring sites and online air pollution monitoring system for total health risk assessment in Hyderabad, India. Int. J. Environ. Res. Public Health. **2**(2), 343–354 (2005)

Arola, A., Lakkala, K., Bais, A., Kaurola, J., Meleti, C., Taalas, P.: Factors affecting short- and long-term changes of spectral UV irradiance at two European stations. J. Geophys. Res. **108**(D17), 4549 (2003). doi:10.1029/2003JD003447

Badarinath, K.V.S., Kharol, S.K., Kiran Chand, T.R., Parvathi, Y.G., Anasuya, T., Nirmala Jyothsna, A.: Variations in black carbon aerosol, carbon monoxide and ozone over an urban area of Hyderabad, India, during the forest fire season. Atmos. Res. **85**, 18–26 (2007a)

Badarinath, K.V.S., Kharol, S.K., Kaskaoutis, D.G., Kambezidis, H.D.: Influence of atmospheric aerosols on solar spectral irradiance in an urban area. J. Atmos. Sol. Ter. Phys. **69**, 589–599 (2007b)

Balis, D.S., Amiridis, V., Zerefos, C., Kazantzidis, A., Kazadzis, S., Bais, A.F., Meleti, C., Gerasopoulos, E., Papayannis, A., Matthias, V., Dier, H., Andreae, M.O.: Study of the effect of different type of aerosols on UV-B radiation from measurements during EARLINET. Atmos. Chem. Phys. **4**, 307–321 (2004)

Barnard, W.F., Saxena, V.K., Wenny, B.N., DeLuisi, J.J.: Daily surface UV exposure and its relationship to surface pollutant measurements. J. Air Waste Manag. Assoc. **53**(2), 237–245 (2003)

Bhattarai, B.K., Kjeldstad, B., Thorseth, T.M., Bagheri, A.: Erythemal dose in Kathmandu, Nepal based on solar UV measurements from multichannel filter radiometer, its deviation from satellite and radiative transfer simulations. Atmos. Res. **85**, 112–119 (2007)

Bigelow, D.S., Slusser, J.R., Beaubien, A.F., Gibson, J.H.: The USDA ultraviolet radiation monitoring program. Bull. Amer. Meteor. Soc. **79**, 601–615 (1998)

Cañada, J., Pedrós, G., Lopez, A., Boscá, J.V.: Influences of the clearness index for the whole spectrum and of the relative optical air mass on UV solar irradiance for two locations in the Mediterranean area, Valencia and Cordoba. J. Geophys. Res. **105**, 4759–4766 (2000)

Chubarova, N.E.: Monitoring of biologically active UV radiation in the Moscow region. Izv. Atmos. Ocean. Phys. **38**(3), 312–322 (2002)

Dahlback, A.: Measurements of biologically effective UV doses, total ozone abundances, and cloud effects with multichannel, moderate bandwidth filter instruments. Appl. Opt. **35**, 6514–6521 (1996)

DeLuisi, J.: Atmospheric ultraviolet radiation scattering and absorption. In: Zerefos, C.S., Bais, A.F. (eds.) Solar Ultraviolet Radiation, Modelling, Measurements, and Effects, NATO ASI Series, vol I 52, pp. 65–84. Springer, Berlin, Germany (1997)

di Sarra, A., Cacciani, M., Campanelli, M., Chamard, P., Cornwall, C., Deluisi, J., Silvestri, L.D., Iorio, T.D., Disterhoft, P., Fiocco, G., Fua, D., Grigioni, P., Junkermann, W., Marenco, F., Meloni, D., Monteleone, F., Olivieri, B.: In: Smith, W.L., Timofeyev, Yu.M. (eds.) Radiation, ozone, and aerosol measurements at Lampedusa during the PAUR II Campaign, IRS 2000: Current Problems in Atmospheric Radiation, pp. 1193–1196. A. Deepak, Hampton, VA (2001b)

di Sarra, A., Cacciani, M., Chamard, P., Cornwall, C., DeLuisi, J.J., Di Iorio, T., Disterhoft, P., Fiocco, G., Fuá, D., Monteleone, F.: Effects of desert dust and ozone on the ultraviolet irradiance at the Mediterranean island of Lampedusa during PAUR II. J. Geophys. Res. **107**(D18), 8135 (2002). doi:10.1029/2000JD000139

Diaz, J.P., Exposito, F.J., Torres, C.J., Carrena, V., Redondas, A.: Simulations of the mineral dust effect on the UV radiation level. J. Geophys. Res. **105**, 4979−4991 (2000)

Elvidge, C.D., Baugh, K.E., Kihn, E.A., Kroehl, H.W., Davis, E.R.: Mapping of city lights using DMSP Operational Linescan System data. Photogramm. Eng. Remote Sensing **63**, 727–734 (1997)

Frederick, J.E., Koob, E.K., Alberts, A.D., Weatherhead, E.C.: Empirical studies of tropospheric transmission in the ultraviolet: broadband measurements. J. Appl. Meteor. **32**, 1883–1892 (1993)

Früh, B., Eckstein, E., Trautmann, T., Wendisch, M., Fiebig, M., Feister, U.: Ground-based measured and calculated spectra of actinic flux density and downward UV irradiance in cloudless conditions and their sensitivity to aerosol microphysical properties. J. Geophys. Res. **108**(D16), 4509 (2003). doi:10.1029/2002JD002933

Gao, W., Slusser, J., Gibson, J., Scott, G., Bigelow, D., Kerr, J., McArthur, B.: Direct-sun column ozone retrieval by the ultraviolet multifilter rotating shadow-band radiometer and comparison with those from Brewer and Dobson spectrophotometers. Appl. Opt. **40**(19), 3149–3155 (2001)

Gies, P., Roy, C., Javorniczky, J., Handerson, S., Lemus-Deschamps, L., Driscoll, C.: Global solar UV index: Australian measurements, forecasts and comparison with the UK. Photochem. Photobiol. **79**, 32−39 (2004)

Harris, N.R.P., Ancellet, G., Bishop, L., Hofmann, D.J., Kerr, J.B., Mcpeters, R.D., Prendez, M., Randel, W.J., Staehelin, J., Subbaraya, B.H., Volz-Thomas, A., Zawodny, J., Zerefos, C.S.: Trends in stratospheric and tropospheric ozone. J. Geophys. Res. **102**, 1571–1588 (1997)

Harrison, L., Michalsky, J., Berndt, J.: Automated multifilter rotating shadow-band radiometer: an instrument for optical depth and radiation measurements. Appl. Opt. **33**, 5118–5125 (1994)

Iqbal, M.: An introduction to solar radiation. Academic Press, New York, 107–128 (1983)

Jaroslawski, J.P., Krzyscin, J.W.: Importance of aerosol variations for surface UV-B level: analysis of ground-based data taken at Belsk, Poland, 1992–2004. J. Geophys. Res. **110**, D16201 (2005). doi:10.1029/2005JD005951

Kalashnikova, O.V., Mills, F.P., Eldering, A., Anderson, D.: Application of satellite and ground-based data to investigate the UV radiative effects of Australian aerosols. Remote Sens. Environ. **107**, 65–80 (2007). doi:10.1016/j.rse.2006.07.025

Kambezidis, H.D., Adamopoulos, A.D., Zevgolis, D.: Spectral aerosol transmittance in the ultraviolet and visible spectra in Athens, Greece. Pure Appl. Geophys. **162**(3), 625–647 (2005)

Kaskaoutis, D.G., Kambezidis, H.D.: The role of aerosol models of the SMARTS code in predicting the spectral direct-beam irradiance in an urban area. Renewable Energy **33**, 1532–1543 (2008)

Kasten, F., Young, A.T.: Revised optical air mass tables and approximation formula. Appl. Opt. **28**, 4735–4738 (1989)

Kharol, S.K., Badarinath, K.V.S.: Impact of biomass burning on aerosol properties over tropical urban region of Hyderabad, India. Geophys. Res. Lett. **33**, L20801 (2006). doi:10.1029/2006gl026759

Kerr, J.B.: Observed dependencies of atmospheric UV radiation and trends. In: Zerefos, C.S., Bais, A.F. (eds.) Solar Ultraviolet Radiation, Modelling, Measurements, and Effects, NATO ASI Series, vol I 52, pp. 65–84. Springer, Berlin, Germany (1997)

Krotkov, N.A., Bhartia, P.K., Herman, J.R., Fioletov, V., Kerr, J.: Satellite estimation of spectral surface UV irradiance in the presence of tropospheric aerosols 1. Cloud-free case. J. Geophys. Res. **103**, 8779–8793 (1998)

Krzyscin, J.W., Puchalski, S.: Aerosol impact on the surface UV radiation from the ground-based measurements taken at Belk, Poland, 1980–1996. J. Geophys. Res. **103**(16), 175–181 (1998)

Lelieveld, J., Dentener, F.J.: What controls tropospheric ozone? J. Geophys. Res. **105**, 3531–3551 (2000)

Levelt, P.F., van den Oord, G.H.J., Dobber, M.R., Mälkki, A., Visser, H., de Vries, J., Stammes, P., Lundell, J., Saari, H.: The ozone monitoring instrument. IEEE Trans. Geosci. Remote Sens. **44**(5), 1093 (2006a)

Levelt, P.F., Hilsenrath, E., Leppelmeier, G.W., van den Oord, G.B.J., Bhartia, P.K., Tamminen, J., de Haan, J.F., Veefkind, J.P.: Science objectives of the ozone monitoring instrument. IEEE Trans Geosci. Remote Sens. **44**(5), 1199 (2006b)

Madronich, S.: UV radiation in the natural and perturbed atmosphere. In: Tevini, M. (ed.) Environmental Effects of Ultraviolet(UV) Radiation, pp. 17–69. Lewis, Boca Raton, FL (1993)

McKenzie, R.L., Paulin, K.J., Dobeker, G.E., Liley, J.B., Sturman, A.P.: Cloud cover measured by satellite and from the ground: relationship to UV radiation at the surface. Int J Remote Sens. **19**, 2969–2985 (1998)

McKenzie, R.L., Aucamp, P.J., Bais, A.F., Björn, L.O., Ilyas, M.: Changes in biologically-active ultraviolet radiation reaching the Earth's surface. Photochem. Photobiol. Sci. **6**, 218–231 (2007)

McKinlay, A.F., Diffey, B.L.: A reference action spectrum for ultraviolet induced erythema in human skin. CIE J. **6**, 17–22 (1987)

Meleti, C., Cappellani, F.: Measurements of aerosol optical depth at Ispra: analysis of the correlation with UV-B, UV-A, and total solar irradiance. J. Geophys. Res. **105**, 4971–4978 (2000)

Meloni, D., di Sarra, A., DeLuisi, J., Di Iorio, T., Fiocco, G., Junkermann, W., Pace, G.: Tropospheric aerosols in the Mediterranean: 2. Radiative effects through model simulations and measurements. J. Geophys. Res. **108**(D10), 4317 (2003a). doi:10.1029/2002-JD002807

Meloni, D., di Sarra, A., Fiocco, G., Junkermann, W.: Tropospheric aerosols in the Mediterranean: 3. Measurements and modeling of actinic radiation profiles. J. Geophys. Res. **108**(D10), 4323 (2003b). doi:10.1029/2002JD003293

Meloni, D., Marenco, F., di Sarra, A.: Ultraviolet radiation and aerosol monitoring at Lampedusa, Italy. Ann. Geophys. **46**(2), 373–383 (2003c)

Meloni, D., Marenco, F., Sarra, A.D.: Ultraviolet radiation and aerosol monitoring at Lampedusa, Italy. Anal. Geophys. **46**(2), 373–383 (2004)

Meloni, D., di Sarra, A., Herman, J.R., Monteleone, F., Piacentino, S.: Comparison of ground-based and Total Ozone Mapping Spectrometer erythemal UV doses at the island of Lampedusa in the period 1998–2003: role of tropospheric aerosols. J. Geophys. Res. **110**, D01202 (2005). doi:10.1029/2004JD005283

Micheletti, M.I., Wolfram, E., Piacentini, R.D., Pazmiño, A., Quel, E., Orce, V., Paladini, A.A.: The incidence of erythemal and UV solar irradiance over Buenos Aires, Argentina. J. Opt. A: Pure Appl. Opt. **5**(5), S262–S268 (2003)

Morys, M., Mims III, F.M., Hagerup, S., Anderson, S.E., Baker, A., Kia, J., Walkup, T.: Design calibration, and performance of MICROTOPS II handheld ozone monitor and Sun photometer. J. Geophys. Res. **106**(D13), 14,573–14,582 (2001)

Ogunjobi, K.O., Kim, Y.J.: Ultraviolet (0.280–0.400 mm) and broadband solar hourly radiation at Kwangju, South Korea: analysis of their correlation with aerosol optical depth and clearness index. Atmos. Res. **71**(3), 193–214 (2004)

Pace, G., Meloni, D., di Sarra, A.: Forest fir aerosol over the Mediterranean basin during summer 2003. J. Geophys. Res. **110**, D21202 (2005). doi:10.1029/2005JD005986

Palancar, G.G., Toselli, B.M.: Erythemal ultraviolet irradiance in Córdoba, Argentina. Atmos. Environ. **36**(2), 287–292 (2002)

Reuder, J., Schwander, H.: Aerosol effects on UV radiation in nonurban regions. J. Geophys. Res. **104**, 4065–4067 (1999)

Schuster, G.L., Dubovik, O., Holben, B.N.: Angstrom exponent and bimodal aerosol size distributions. J. Geophys. Res. **111**, D07207 (2006)

Singh, S., Singh, R.: High-altitude clear-sky direct solar ultraviolet irradiance at Leh and Hanle in the western Himalayas: observations and model calculations. J. Geophys. Res. **109**, D19201 (2004). doi:10.1029/2004JD004854

Udelhofen, P.M., Cies, P., Roy, C., Randel, W.J.: Surface UV radiation over Australia, 1979–1992: effects of ozone and cloud cover changes on variations of UV radiation. J. Geophys. Res. **104**, 19135–19159 (1999)

WHO: Global Solar UV Index: A Practical Guide. World Health Organization, Geneva (2002)